

Glacial geomorphology and paleoglaciation patterns in Shaluli Shan, the southeastern Tibetan Plateau – Evidence for polythermal ice cap glaciation

Ping Fu ^{a,*}, Jonathan M. Harbor ^b, Arjen P. Stroeven ^a, Clas Hättestrand ^a, Jakob Heyman ^b, Liping Zhou ^c

^a Department of Physical Geography and Quaternary Geology, Stockholm University, Stockholm 10691, Sweden

^b Department of Earth and Atmospheric Sciences, Purdue University, West Lafayette, Indiana 47906, USA

^c College of Urban and Environmental Science, Peking University, Beijing, 102413, China

ARTICLE INFO

Article history:

Received 8 May 2012

Received in revised form 24 October 2012

Accepted 25 October 2012

Available online 2 November 2012

Keywords:

Glacial landform

Geomorphological mapping

Polythermal ice cap

Tibetan Plateau

ABSTRACT

Glacial geomorphological mapping from satellite imagery and field investigations provide the basis for a reconstruction of the extent and style of glaciation of the Shaluli Shan, a mountainous area on the southeastern Tibetan Plateau. Our studies provide evidence for multiple glaciations, including the formation of regional ice caps and valley glaciers. The low-relief topography within the Shaluli Shan, the Haizishan Plateau, and Xinlong Plateau display zonal distributions of glacial landforms that is similar to those imprinted by Northern Hemisphere ice sheets during the last glacial cycle, indicating the presence of regional, polythermal ice caps. Abundant alpine glacial landforms occur on high mountain ranges. The pattern of glaciated valleys centered on high mountain ranges and ice-scoured low relief granite plateaus with distinctive patterns of glacial lineations indicate a strong topographic control on erosional and depositional patterns by glaciers and ice caps. In contrast to the Shaluli Shan, areas farther north and west on the Tibetan Plateau have not yielded similar landform evidence for regional ice caps with complex thermal basal conditions. Such spatial differences across the Tibetan Plateau are the result of variations in climate and topography that control the extent and style of glaciations and that reinforce the importance of detailed geomorphological mapping for understanding paleoclimate variations and characteristics of former glaciations.

© 2012 Elsevier B.V. All rights reserved.

1. Introduction

Considerable controversy and uncertainty have surrounded reconstructions of the extent, timing, and landscape impact of Tibetan Plateau glaciations. Resolving this controversy is important because of the central role of glaciation in paleoclimate reconstructions and geological evolution models. In some of the earliest studies, Hedin (1909, 1922) and Ward (1922, 1934) argued against the presence of a former ice sheet on the Tibetan Plateau mainly because of the lack of till, glacial sediments typically deposited by continental ice sheets elsewhere. Huntington (1906), Trinkler (1930), and Sinitsum (1958), on the other hand, argued for the former presence of a continental-scale ice sheet in this region based on inferred glacial origins of large lakes on the plateau. A series of major expeditions to the Tibetan Plateau conducted by Chinese scholars in the 1950s, 1960s, and 1970s produced a large number of papers that presented evidence for glacier expansions during the Pleistocene characterized by ice caps, trellis valley glaciers and piedmont glaciers, and these papers contradicted the ice sheet hypothesis (Luo and Yang, 1963; Cui, 1964; Shi and Liu, 1964; Li, 1975;

Zheng and Shi, 1976; Cui, 1979; Zheng and Li, 1981; Shi et al., 1982; Li and Xu, 1983; Li et al., 1983; Shi et al., 1986). In the 1980s and 1990s, Kuhle (1986, 1987, 1988, 1990, 1991, 1995) resurrected the ice sheet hypothesis and argued for a significant plateau-wide ice sheet during the Last Glacial Maximum (LGM). This stimulated a renewed interest for studies of glacial chronologies in key locations. These studies indicated that a variety of deposits and landforms had been misinterpreted as glacial landforms (Derbyshire et al., 1991; Shi, 1992; Zheng and Rutter, 1998). Thus, most researchers now recognize that expansions of ice during the Pleistocene were limited, predominantly as glaciers and ice caps radiating from the highest mountains, and that the timing of these events sometimes shows a mismatch with the northern hemispheric ice sheet records (Zheng, 1989; Rutter, 1995; Owen et al., 2002, 2005; Zheng et al., 2002; Lehmkuhl and Owen, 2005; Shi et al., 2005; Heyman et al., 2009, 2011a, 2011b). The most comprehensive reconstruction of glacial extent on the Tibetan Plateau indicates that at most approximately $0.5 \times 10^6 \text{ km}^2$ was covered by glacier ice (Li et al., 1991).

Although several comprehensive assessments of existing reconstructions provide an overall picture of Quaternary glaciations (Li et al., 1991; Shi et al., 1992, 2005), much work is still required to systematically determine the extents, timing, and impacts of glacial advances, particularly as the responses of glaciers to past climate change seem to have varied in their timing and extent across the Tibetan Plateau

* Corresponding author. Tel.: +46 8164728; fax: +46 8164818.

E-mail address: ping.fu@natgeo.su.se (P. Fu).

(Owen et al., 2005, 2008). Most reconstructions have focused on the use of individual landforms, primarily moraines and glacial valleys, to delineate glacial extent (Cui, 1981a; Derbyshire et al., 1991; Lehmkuhl and Liu, 1994; Zheng and Rutter, 1998; Zheng, 2000, 2001; Zheng et al., 2002; Owen et al., 2003; Klinge and Lehmkuhl, 2004; Zhou et al., 2007; Wang et al., 2011), while fewer studies have examined broader suites of glacial landforms (Cui, 1981b; Zheng and Ma, 1995). However useful these studies are, detailed and consistent studies of the pattern of glaciations from glacial landforms are lacking for large parts of the Tibetan Plateau.

To produce regional reconstructions of glacial extent based on detailed glacial geomorphology and chronology for large regions of the Tibetan Plateau, an international team has been conducting three consecutive projects focused on the Bayan Har Shan (Heyman et al., 2008), Tanggula Shan (Morén et al., 2011), and Shaluli Shan (Fu et al., 2012) (Fig. 1). This includes detailed and consistent mapping work that provides a basis for an analysis of the types and patterns of landforms aimed at understanding the extent and dynamics of the glaciers that produced them. For example, studies of the landforms of the Bayan Har Shan (Heyman et al., 2008, 2009; Stroeven et al., 2009) have shown that there were ice field- and valley glacier-style glaciations during the Pleistocene. However, they found no evidence that the area was ever covered by a Huang He Ice Sheet as proposed by Zhou and Li (1998). Given the vast area of the Plateau, more detailed and consistent mapping is required for other areas before a detailed picture can emerge of the extent and pattern of Quaternary glaciation on the Tibetan Plateau.

Building on detailed geomorphological mapping (Fu et al., 2012), here we examine the types and patterns of glacial landforms in the Shaluli Shan region, in particular the landform patterns across the Haizishan Plateau. We interpret patterns of glacial lineations, scoured

terrain, and relict areas in terms of basal ice thermal condition, and discuss why this region displays different landform assemblages than other areas of the Tibetan Plateau that have been studied in similar detail.

2. Physical setting

The study area of 104,000 km² is situated on the southeastern margin of the Tibetan Plateau and includes the Shaluli Shan (Shan = mountain range) and a series of other NW–SE trending mountain ranges (Fig. 1). These mountains compose the eastern part of Hengduan Mountain, which is one of the most prominent ranges of the Tibetan Plateau. Whereas uplift of the Tibetan Plateau began around 50 million years ago (Harrison et al., 1992), based on thermochronological data it has been argued that the southeastern Tibetan Plateau experienced rapid uplift during the late Cenozoic (Clark et al., 2005; Ouimet et al., 2010). The bedrock geology consists mainly of Triassic flysch of the Songpan-Garze terrane and Triassic volcanic and sedimentary rocks, intruded by Jurassic plutons (Ouimet et al., 2010). The two major granite plutons underlie two very distinctive geomorphological units in this area, the Haizishan Plateau and the Xinlong Plateau.

The Shaluli Shan area includes both high relief mountains and relatively low relief upland landscapes. The mountains are deeply incised by major river branches, while low relief landscapes in between display little incision by small tributaries. The plateau-elevation primarily ranges between 3500 and 4800 m above sea level (asl), with the highest peak reaching 7556 m asl (Mt. Gongga). The major rivers cut deep into the high relief mountains – in some cases down to 2000 m below the mountain peaks creating a local relief of up to 5000 m over a 15-km distance.

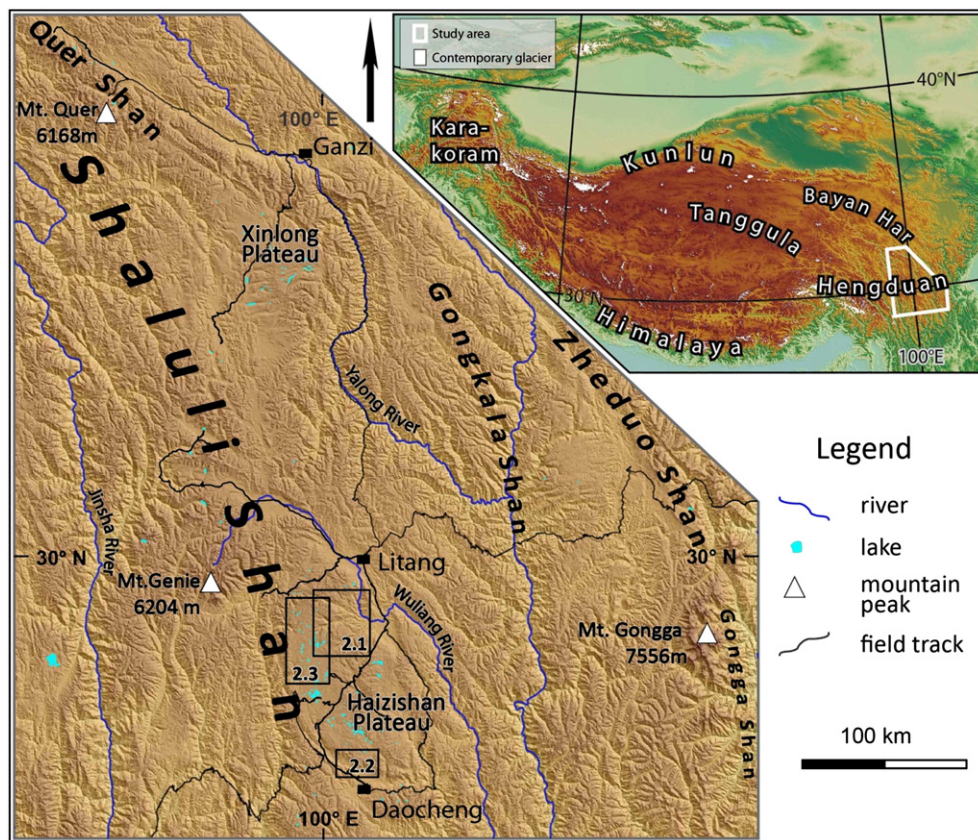


Fig. 1. Location and topographic map of the Shaluli Shan area. Locations of Figs. 2.1, 2.2, and 2.3 are indicated with black rectangles. Field investigations along roads and in key areas were carried out in 2008, 2009, and 2011. Digital elevation model from Jarvis et al. (2008), lake polygons from U. S. Geological Survey (<http://www.usgs.gov/>), and rivers from National Geomatics Center of China (<http://ngcc.sbsm.gov.cn/english/about.asp>). Modern glaciers for the inset are derived from GLIMS (<http://www.glims.org>).

Climate is strongly influenced by the summer monsoon system, which accounts for over 90% of the annual precipitation of 300–1000 mm (Shi et al., 2006). Abundant glacial landforms indicate that this area was extensively glaciated during the Quaternary (Zheng, 2006). However, only a few glaciers remain in the area today, primarily in Gongga Shan, Genie Shan, and Quer Shan.

3. Glacial history of the southeastern Tibetan Plateau and the Shaluli Shan area

Because of its location across the monsoon track and the dramatic altitudinal range, the southeastern part of the Tibetan Plateau (the Hengduan Mountains; Fig. 1) receives abundant precipitation, which favors the growth of glaciers. The past extent of glaciers in the Hengduan Mountains, reconstructed based on glacial landforms and sediments, indicates that this was one of the most extensively glaciated area of the Tibetan Plateau during the Quaternary (Shi et al., 2006). Previous studies have suggested that a deeply weathered ridge on the southwestern margin of the Haizishan Plateau locally constrains the extent of the oldest glaciation in the region – the Daocheng glaciation (Li et al., 1991, 1996). The timing of this glaciation during marine oxygen isotope stage (MIS) 16 is based on electron spin resonance (ESR) ages from Xu and Zhou (2009). This is consistent with identification of early glaciations in other areas of the plateau, based on geomorphology and stratigraphy (Zheng and Shi, 1976; Li and Xu, 1983; Zheng, 2002). From red weathering products on this ridge, that are believed to have been formed at lower altitudes in sub-tropical climate conditions, Li et al. (1996) inferred that this region was uplifted 1200 m to its present elevation since the interglacial equivalent to MIS 13 (Shi et al., 2011). Based on geomorphological records Li et al. (1996) also identified two younger glaciations, locally named the Rongbacha and Zhusiqin glaciations in the Shaluli Shan region, and assigned these to Penultimate and Last Glaciation ages based on morphostratigraphical evidence.

In reconstructing the chronology of past glacier expansions in Shaluli Shan, earlier studies have mainly relied on radiocarbon (^{14}C), thermoluminescence and ESR dating for late Pleistocene glaciations (Li et al., 1983; Zheng and Ma, 1994; Lehmkuhl et al., 1998; Zheng, 2000, 2001; Xu and Zhou, 2009). More recently, cosmogenic nuclide exposure dating and optically stimulated luminescence ages from the Shaluli Shan and Gongga Shan have been used to provide age control for deposits related to MIS 2 and MIS 1 glaciations in this area (Schäfer et al., 2002; Owen et al., 2005; Wang et al., 2006; Zhou et al., 2007; Graf et al., 2008; Strasky et al., 2009; Xu et al., 2010). Wang et al. (2006) provided bedrock exposure ages indicating glaciation at MIS 6 and a boulder exposure age in the deeply weathered ridge of 421–726 ka with erosion correction and uplift rate adjustment.

Previous studies of the glacial geomorphology of the Shaluli Shan have identified landforms and deposits related to regional ice caps and extensive valley glaciers (Li et al., 1991; Zheng and Ma, 1995; Li et al., 1996; Zheng, 2001). Li et al. (1996) reconstructed a paleo Daocheng ice cap in Haizishan Plateau covering 3600 km² with a thickness up to 800 m during the maximum glaciation. Using an accumulation-area ratio approach with positions of terminal moraines and glacial cirques, they calculated the depression of paleo equilibrium line altitudes for the oldest glaciation, Penultimate, and Last Glaciation as 800 m, 650 m, and 450 m, respectively. Zheng and Ma (1995) provided detailed descriptions of glacial landforms formed by the Daocheng ice cap on the Haizishan Plateau, including glacial troughs and basins, roche moutonnées and drumlins. They also identified four zones of landforms: a central zone of limited erosion landforms, an intermediate zone of moderate erosional landforms, a zone of strong erosional activity, and finally an outer depositional landform zone. They suggested that the most distinct moraines in the outlet valleys were LGM in age, that less prominent ridges distal to these moraines were remnants of the middle Pleistocene, and that a till platform is evidence of the oldest and most extensive glaciation in this region. Although studies by

previous workers (Zheng and Ma, 1995; Li et al., 1996) have provided important insight into the glacial history for some key locations in the study area, here we aim to produce a more comprehensive and systematic reconstruction of the glacial geomorphology of the Shaluli Shan area based on detailed glacial landform mapping.

4. Methods

4.1. Geomorphological mapping

Initial mapping was performed principally using the Shuttle Radar Topography Mission digital elevation model (DEM) of 90 m horizontal resolution (Jarvis et al., 2008) and orthorectified Landsat ETM + imagery with 15-m horizontal resolution (GLCF, 2011). The DEM was processed using ArcGIS 9.3 to produce shaded relief images that were overlain semi-transparently on the DEM to enhance the visual impression of the topography. Orthorectified Landsat ETM + imagery was processed using ERDAS to produce composite images of bands 5, 4, 2 and 4, 3, 2 (30-m resolution) draped with semitransparent gray-scale images of band 8 (15-m resolution). Mapping based on operator interpretation of these remote-sensing products was performed using the Editor tool in ArcMap, and Google Earth was used for three-dimensional landform visualization. The mapping results were then checked using detailed field investigations over the course of three field seasons, focusing on key areas for paleoglaciological reconstruction. The mapping work has generated a detailed glacial landform map of the Shaluli Shan area and the method for mapping is described in detail in Fu et al. (2012).

Five types of glacial landforms were identified in the study area. A glacial valley is identified by its distinct U-shaped cross section and smooth valley sides that result from the erosion and eradication of interlocking valley spurs, which contrasts with the V-shaped valley cross section and interlocking spurs typical of fluvial incision (Fig. 2A,B,C). The upper boundary of the U-shaped valley is normally represented by an abrupt change in slope that can be identified from the DEM and Google Earth. Marginal moraines are arc-shaped ridges that run across the valley or on the plateau surface, or are slightly curved ridge features located on the valley sides (Fig. 2D, E). They can be identified from Landsat images and Google Earth. Hummocky terrain, an irregularly shaped sedimentary deposit exhibiting a typical surface expression of hills and mounds (Benn and Evans, 2010), predominantly occurs along valley sides and across valleys. Glacial lineations are elongated landforms (Fig. 2F, H) that usually occur in clusters and that normally are clearly visible on Landsat imagery and in Google Earth. Scoured terrain consists of low-relief, bedrock-dominated surfaces with rock basins and intervening rock knobs (Benn and Owen, 1998) and is typically dotted with lakes (Fig. 2F, G).

4.2. Field studies

Field studies to check and refine the geomorphological mapping for key areas were conducted during 2008, 2009, and 2011 (field route is shown in Fig. 1). We used handheld GPS units to locate point features and boundaries and checked our remote-sensing-based mapping with ground-based observations of landforms and sediment sections. We identified some deposits that could not be seen on the imagery because of scale or vegetation. This included observations of dispersed boulders and glacial till that were used to infer the former extension of the ice cap beyond the most distal moraine position. Natural and man-made sections allowed us to confirm some deposits as being diamictites of glacial origin, whereas some roadcuts exposed saprolite sections indicating areas of limited erosion.

5. Results

Our geomorphological mapping provides the most detailed and comprehensive map of glacial landforms of the Shaluli Shan area to date (Fu et al., 2012). Abundant glacial landforms are found on the

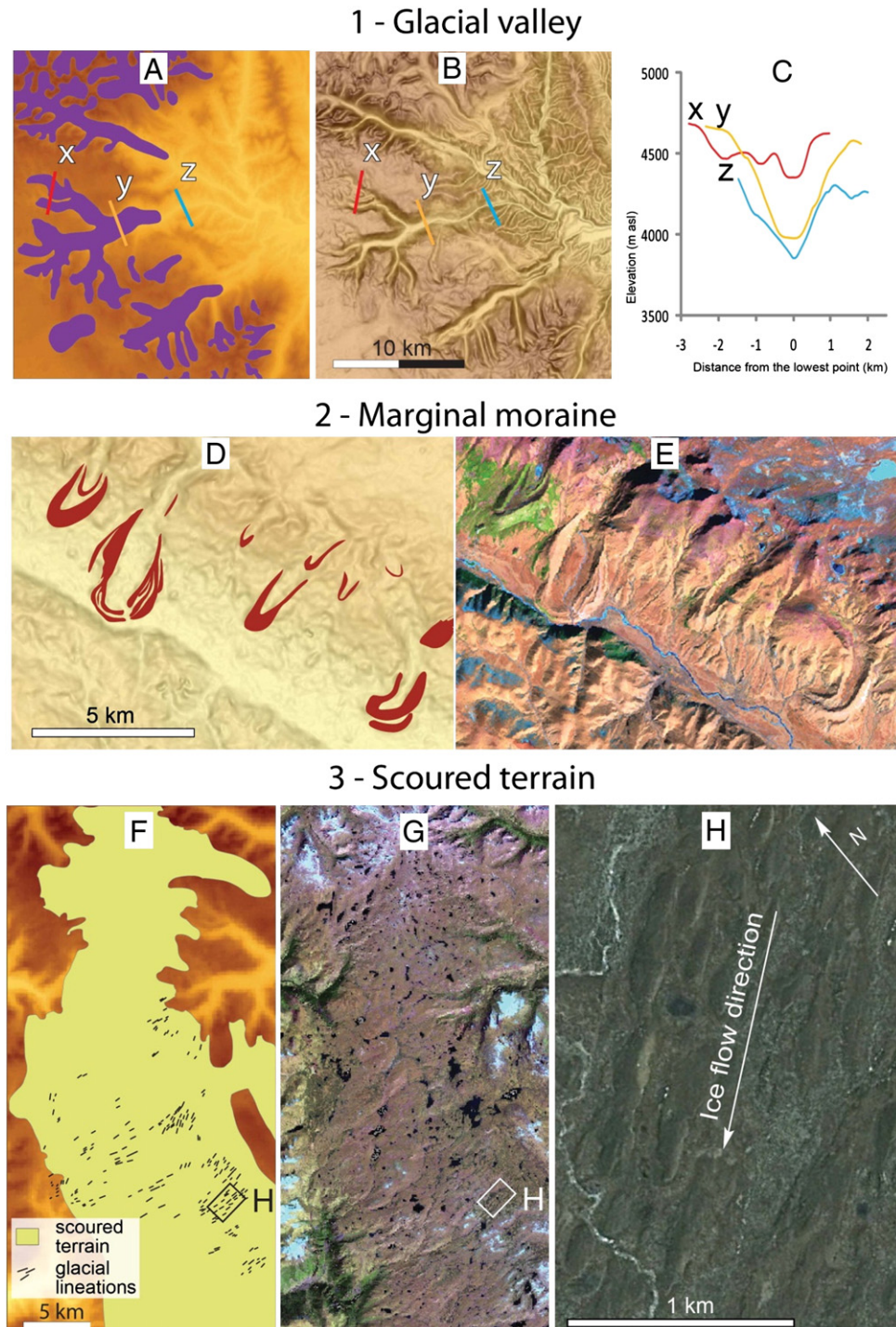


Fig. 2. Landform recognition from remotely sensed images. (1) Glacial valley as (A) mapped on DEM, (B) seen on the DEM draped with a slope image, and (C) in cross-profile, where glacial U-shaped sections (x, y) differ from V-shaped sections (z); (2) marginal moraine as (D) mapped on DEM and (E) seen on Landsat image; and (3) scoured terrain and lineations as (F) mapped on DEM and seen on (G) Landsat image and (H) Google Earth. Panel (H) is indicated in panel (F) and (G). All the areas depicted are shown in Fig. 1 (adapted from Fu et al., 2012).

present ice-free areas, including distinctive patterns of glacial valleys, marginal moraines, hummocky terrain, scoured terrain, and glacial lineations (Fig. 3).

5.1. Glacial landforms related to valley glaciation

Extensive glacial landforms related to valley glaciation are found in the study area, including glacial valleys, cirques, marginal moraines,

and hummocky terrains. These features are most common in areas centered on high mountain ranges, including the Gongga Shan, the Genie Shan, and the Quer Shan (Figs. 3, 4). Glacial valleys have distinct U-shaped cross-profiles, usually with a distinctive cirque at the valley head (Fig. 4B). The easterly facing glacial valleys are longer than the westerly facing valleys in the southern part of the study area (Gongga Shan, Haizishan, Genie Shan); while in the northern part of the study area, north-facing valleys are longer than south-facing valleys (Quer

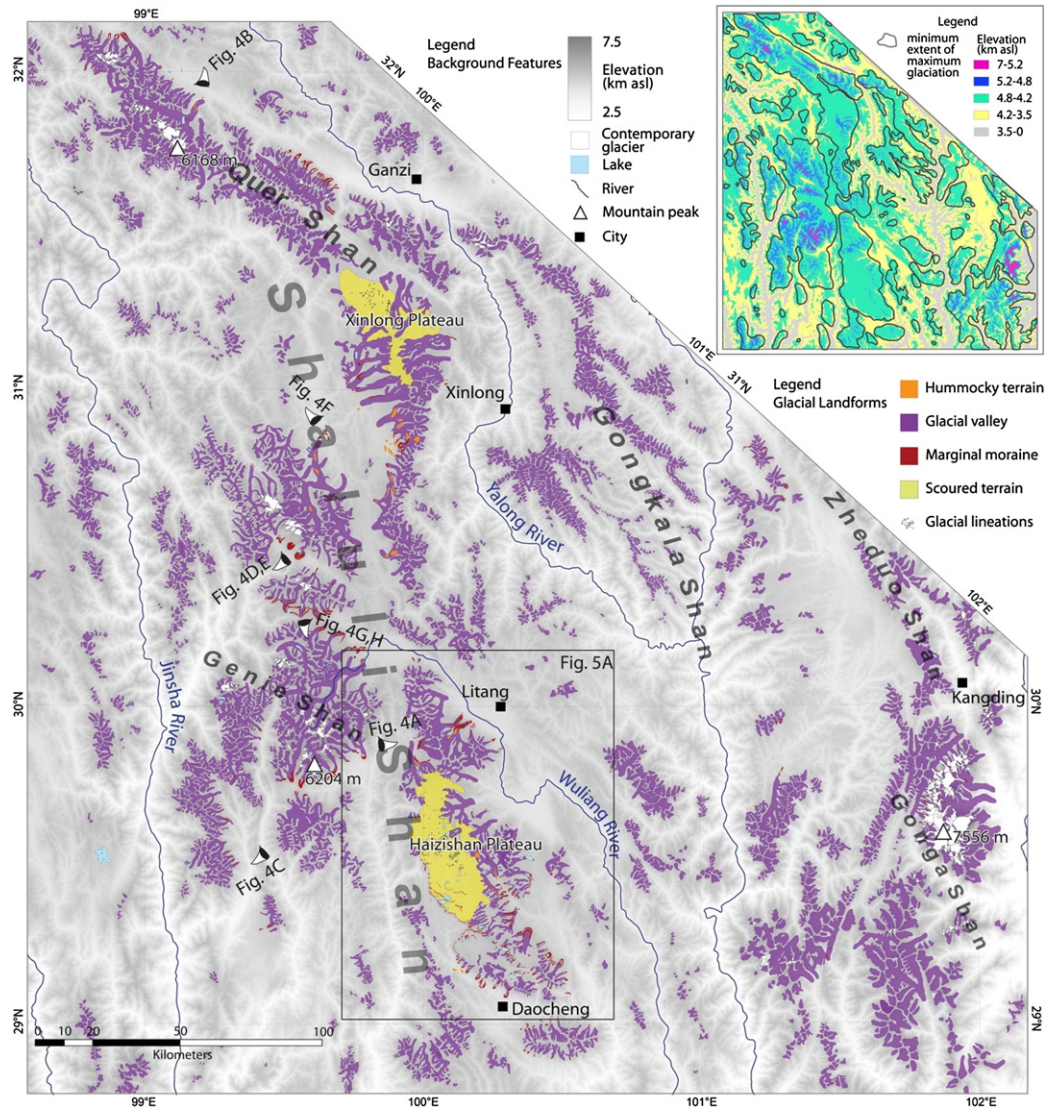


Fig. 3. Detailed glacial landform map of the Shaluli Shan area (Fu et al., 2012). The inset map displays the outline of the minimum extent of maximum glaciation projected on the DEM (Fig. 10B). The glaciated area was reconstructed based on the distribution of glacial landforms and field observations of glacial deposits, such as the dispersal of erratics (cf. Heyman et al., 2009). The locations and viewing directions of Figs. 4A–H and 5A are depicted.

Shan). Ice-marginal moraines include end moraines and lateral moraines (Fig. 4D, E, F), which, in some locations, are exceptionally long. Those long marginal moraines are primarily found in the Shaluli Shan and range up to 25 km in length (Fig. 4G, H). Seventy-three hummocky terrain polygons were mapped in the study area. It is a rather minor component in this landscape, and hummocky terrain is found primarily in wide valleys and at the mouths of glacial valleys.

5.2. Glacial landforms of the low relief plateaus

In addition to glacial landforms related to valley glaciation, which are ubiquitous in the Himalaya and other mountain ranges on the Tibetan Plateau, unique glacial landforms and landform assemblages occur on the Haizishan Plateau and the Xinlong Plateau. Compared to the Xinlong Plateau, the Haizishan Plateau has a more well-developed landform pattern indicating a more geomorphologically active ice cap glaciation or better landform preservation.

The Haizishan Plateau (Fig. 1) formed on a Jurassic granite Pluton that has intruded Triassic metamorphic sedimentary rock. The plateau surface elevation is above 4200 m asl, with higher topography in the central zone and in the north reaching above 4600 m asl. Although

glaciers are absent from the plateau, glacial landforms are abundant (Fig. 5).

5.2.1. Glacial valleys and moraines

The U-shaped valleys without cirques at their heads cut deeply into the margin of the Haizishan Plateau. The largest U-shaped valleys are closest to the highest elevation area (4600–5000 m asl; Fig. 6A), where they are up to 18 km long, 3 km wide and 500 m deep. The U-valleys on the west side of the plateau are narrower and shorter (Fig. 6C). Numerous marginal moraines are present, including arc-shaped lateral or lateral-terminal moraines in valleys and sinuous moraines on the plateau surface (Fig. 6C, D, E). Commonly, the Haizishan Plateau and the glacial valleys that are incised into its margins have three sets of moraines extending radially out from the plateau. The most distal moraine complex is also the best developed and is normally located at the mouth of glacial valleys (Fig. 6C). It can include up to five distinctive ridges, such as the moraine complex close to the village of Kuzhaori (Fig. 5A), but often the ridges overlap each other. The intermediate set of moraines is less prominent than the outermost one and often contains two or three ridges (Fig. 6D). These moraines are located 7–8 km and 3–4 km up valley from the most distal moraines in large

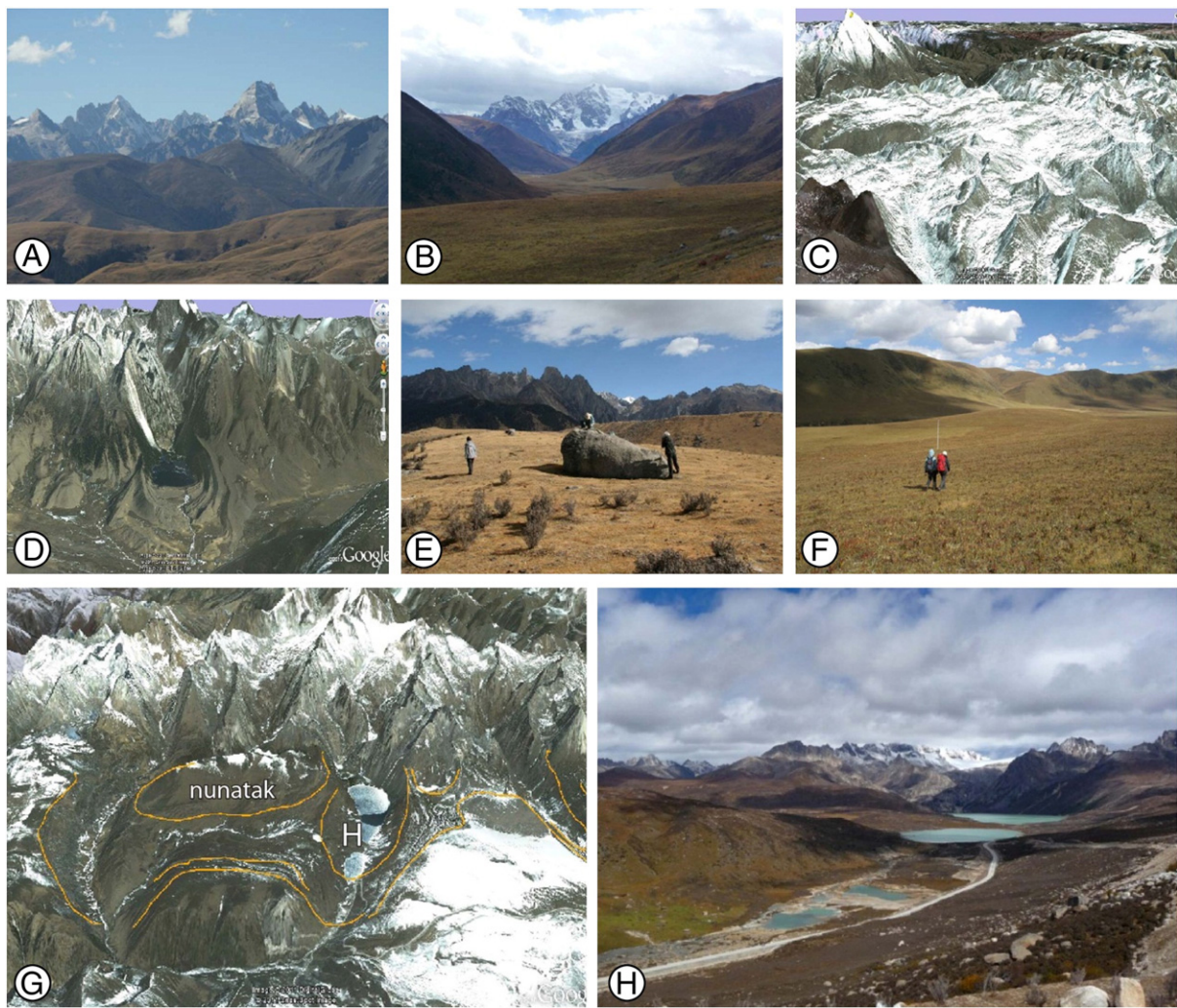


Fig. 4. Landforms formed by alpine glaciers in the study area. (A) Cirques and horns; (B) glacial valley; (C) Google Earth image of an eroded valley heads; (D) Google Earth image of moraines with sharp crests; (E) moraine with large boulder; (F) moraine with very gentle slope; (G) Google Earth image of piedmont glacier moraine and nunatak (yellow lines delineating moraines); and (H) field photo of valley H in panel (G). Location and viewing angle of the images are given in Fig. 4.

valleys and small valleys, respectively. The most proximal set of moraines occurs in valleys to the east and north and on the plateau (west and south sectors), where they form three distinct and sinuous ridges. The most distal of these three ridges can be traced for 50 km, and field investigation revealed that large boulders associated with this moraine also occur dispersed beyond the moraine ridge (Figs. 5A, 6E). Detailed field mapping of boulders and till remnants near the village of Sangdui similarly indicate that boulders occur beyond the most distal moraines and are dispersed across the main valley and halfway up the opposite mountain slopes (Figs. 6F, G; green dots in Figs. 5A, C).

5.2.2. Scoured terrain, lineations, and saprolites

A large area of scoured terrain was mapped on the low relief plateau surface, consisting of a knock and lochan landscape with numerous rock basins and intervening rock knobs, resulting in a widespread occurrence of lakes (Figs. 5, 6H, I, J, L). Boulders of local origin are abundant in this area, while erratics occur more sparsely. Two sets of striation directions (E–W and NE–SW) were observed on polished bedrock on the eastern plateau (Fig. 6K). Furthermore, numerous lineations were mapped in the region characterized by scoured terrain (Fig. 5A). These lineations range from 70 to 1000 m in length. They cluster together and are aligned parallel or subparallel to each other and, in some cases, have a slightly radiating pattern at the mouth of a valley or

converge toward the head of a valley. The main cluster of mapped lineations is in a W–E direction, consistent with one of the directions of striations found on the polished bedrock. They are primarily located close to the central area of the Haizishan Plateau. Most of them have flat top surfaces and low length/width ratios ≥ 1.5 . However, the lineations are more elongated farther away from the central plateau area. Field observations showed that the mapped lineations close to the central area are primarily composed of thick till; and the more elongated ones located farther away from the central area are composed of till draped over a bedrock core.

To the east of the lineations, it is a narrow zone of higher topography with few erosional and depositional landform features mapped and tors presented (Fig. 6M). This zone is coincident with an elongated area of metamorphic sedimentary bedrock (Fig. 5A). To its east, the elevation falls rapidly as several large valleys have been deeply incised into the plateau margin. In the scoured terrain area and close to the divide in northern Haizishan Plateau, saprolite profiles are found several meters thick and overlain by a 20–30 cm thick regolith layer of colluvial origin. The presence of saprolites seems to confirm that there was little or no glacial erosion in some places in the scoured terrain and close to the central region (s1 and s2 in Figs. 5A, 6N). A similar pattern of erosion and preservation, including occurrences of saprolite, also exists on the Xinlong Plateau (Figs. 3, 6J, O).

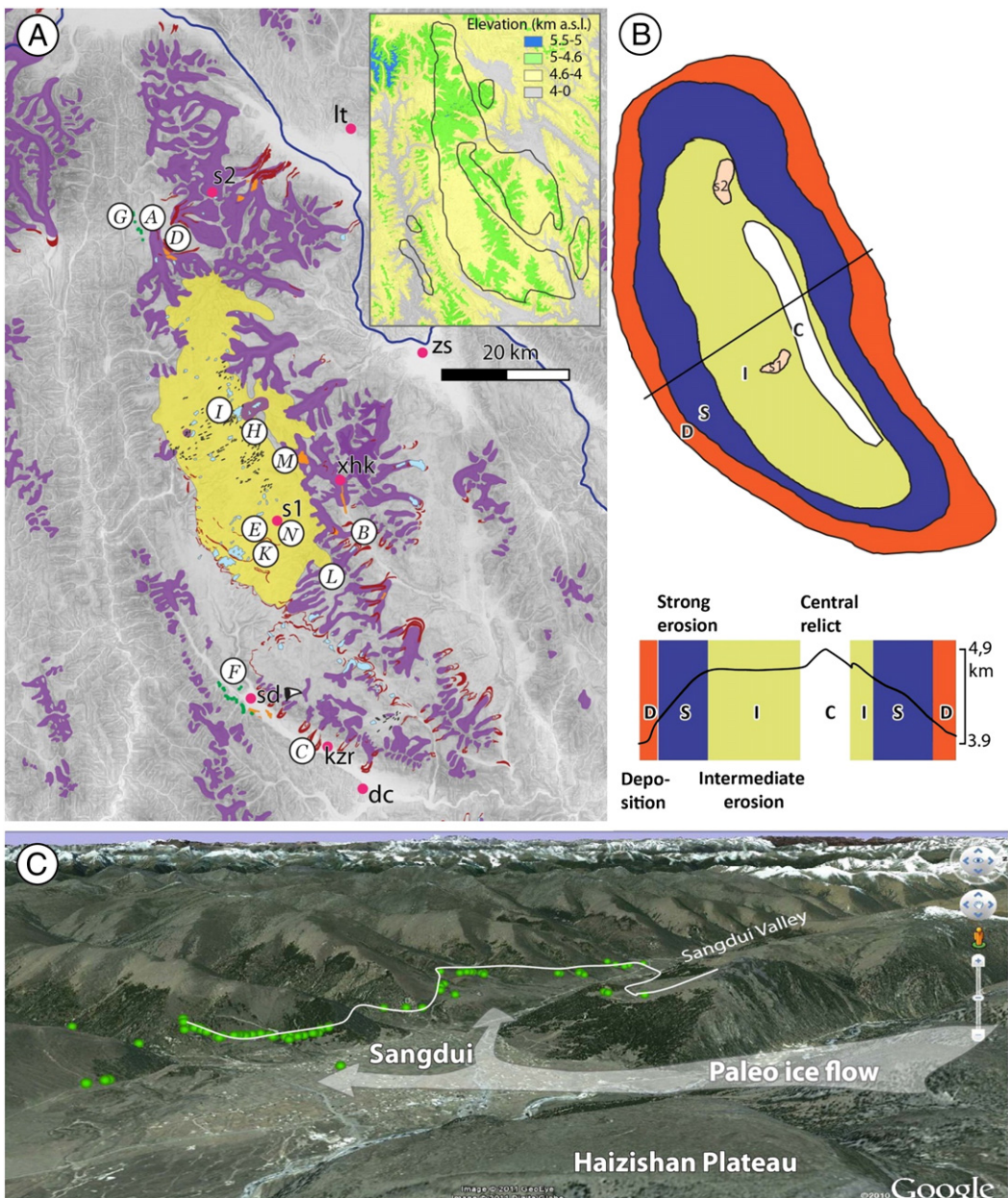


Fig. 5. Glacial landforms of the Haizishan Plateau. (A) Detailed glacial landform map of the Haizishan Plateau. The circled letters are sites of photos of panels A–I and K–N in Fig. 6. Place labels: dc—Daocheng, lt—Litang, sd—Sangdui, and xhk—Xiaohekou. Locations s1 and s2 denote the two positions of saprolite profiles. The inset shows the DEM with granite bedrock delineated as black polygons. (B) A sketch map and cross-profile of the zonation of landforms formed by the Haizishan ice cap. Capital letters denote D—depositional zone, S—zone of strong erosion, I—the zone of intermediate erosion, and C—the central area with minimum erosion. Saprolite locations (inside the pink polygons) are labelled s1 and s2. (C) Reconstruction of paleo ice flow and ice extent in Sangdui area. A viewing angle is given in panel (A) next to the text-sd. The green dots are GPS records of the highest occurrence of erratics, outlining the margin (white line) of the maximum extent of the Haizishan ice cap. During maximum glaciation, the ice may have dammed a lake in the Sangdui valley.

6. Interpretation

Two types of glacial landform assemblages — related to alpine style and ice cap style glaciation, respectively — are located primarily above 4000 m asl in high mountain areas and low relief plateaus. Some marginal imprints — such as the end of glacial valleys, moraines, and glacial boulders — extend down to 3500 m asl.

For alpine glacial landforms, glacial valleys are widely distributed; and the larger of these, exceeding 20 km in length, are concentrated in mountain massifs above 5200 m asl in elevation. Around some of the very high peaks the walls between cirques have been eroded, indicating that glaciers were once connected to form small ice fields

(Fig. 4C). Glaciers extending from such ice fields were up to 45 km long, 3 km wide, and 400 m thick based on the height from the glacial valley bottom to valley shoulder. In some locations, glaciers from adjacent valleys merged to produce exceptionally long glaciers and marginal moraines with patterns that indicate that some intervening areas were completely engulfed by glacier tongues, forming nunataks (Figs. 4G, H). Moraines are mainly located in areas above 4100 m asl, where chances are higher to survive from post-glacial fluvial erosion than at lower elevations.

The patterns of glacial landforms in Haizishan Plateau indicate the existence of ice caps or ice fields at multiple stages, which at the maximum stage covered the entire Haizishan Plateau and reached down

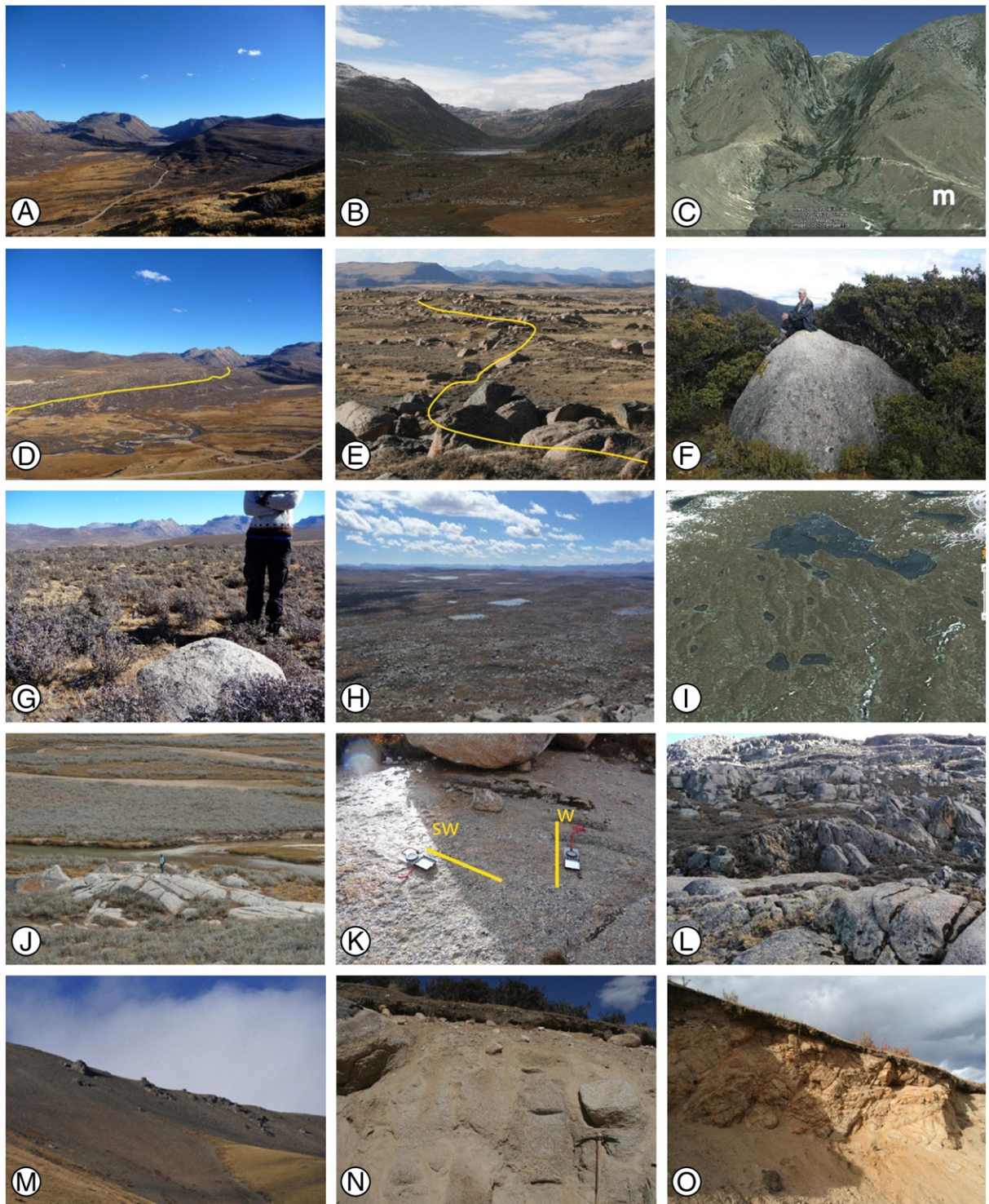


Fig. 6. Images of landforms associated with the Haizishan and Xinlong ice caps. For locations of the panels A–I and K–N on the Haizishan Plateau, see Fig. 5A. (A, B) Glacial valley; (C) Google Earth image of a glacial valley and the most distinctive and outmost set of moraines (label as m); (D) the intermediate set of moraines delineated by yellow line; (E) the innermost set of moraines denoted by concentrated boulder lines in yellow; (F) dispersed boulder on the west part of the Haizishan Plateau; (G) dispersed boulders on the north part of the Haizishan Plateau; (H) rock basins and lineations in the central Haizishan Plateau; (I) Google Earth image of lineations; (J) roche moutonnée on the Xinlong plateau; (K) two sets of striations (yellow lines indicate axis of ice flows); (L) rock steps; (M) central relict ridge with tors; (N) saprolite profile in the Haizishan Plateau; and (O) saprolite on the Xinlong Plateau.

to the surrounding lowlands. During maximum glaciation, the cross-valley ice flow in Sangdui may have produced glacier-dammed lakes in the main Sangdui valley (Fig. 5C). Numerous marginal moraines, including arc-shaped lateral or lateral-terminal moraines in valleys and sinuous moraines on the plateau surface, can be used to initially define the extent of the ice cap and outlet glaciers. However, the maximum area of ice

extent can be extended if the distributions of glacial boulders and till remnants found outside the mapped moraines are added. Based on the distribution of glacial deposits and landforms, the reconstructed Haizishan ice cap had an area of 4000 km² during its maximum stage. Scoured terrain has rarely been observed on the Tibetan Plateau previously but can be found in a few places in the Shaluli Shan. Scoured terrain

and glacial lineations are typical landforms associated with warm-bed areas under large ice caps or ice sheets. They have been mapped in areas formerly covered by the Scandinavian and Laurentide ice sheets and used to reconstruct paleo ice sheet basal thermal regimes (Sugden and Watts, 1977; Boulton and Clark, 1990; Kleman et al., 2008).

The presence of well-preserved saprolites and the central limited erosion zone on a plateau surface where evidence of ice cap glaciation is present indicates that some areas were consistently protected by cold-based ice. Saprolite development elsewhere usually takes millions of years, which requires long-term tectonic stability, moderate relief and warm climate (Lidmar-Bergström, 1995; Butt et al., 1997). Though solute weathering could accelerate the weathering process (Brantley and White, 2009), it is not likely that the saprolite on the two plateaus developed after the last glaciation, as boulders and pebbles in the overlying till layers show no extensive weathering features. This indicates that the saprolite here at least escaped glacial erosion during the last glaciation. The juxtaposition of extensive landscapes with erosional landscapes indicates a subglacial boundary between areas of different basal thermal properties as part of an ice mass with both warm-based and cold-based conditions.

7. Discussion

7.1. Zonation of glacial landforms on the Haizishan Plateau

The Haizishan Plateau was covered by an ice cap whose existence was already proposed by previous Chinese studies (Zheng and Ma, 1995). Distinct zones of glacial landform associations were identified

on the Haizishan Plateau (Figs. 5B, 7). The outermost zone is depositional and includes numerous moraines formed by outlet valley glaciers. Inside the depositional zone is a zone characterized by strongly eroded glacial valleys separated by unmodified plateau surfaces or bedrock ridges. These unmodified surfaces may have been nunataks or subglacial areas of little or no erosion. The zone of strong valley erosion is associated with outlet glaciers and has many features associated with landscapes of selective linear erosion (Sugden and John, 1976; Stroeven et al., 2011) – in which preferential erosion in deeper valleys beneath an ice sheet/ice cap occurs where ice is thick and ice flow fast – and intervening areas where ice is absent or thin and frozen to its base. Apparently, therefore, certain pre-glacial fluvial valleys along the plateau margin became primary passages for outlet glaciers from the plateau ice cap, and with localized high ice flow velocities these were also sites of preferential erosion. Unmodified or little modified plateau surfaces and bedrock ridges draped with erratic boulders between the valleys indicate that the interfluves were ice-covered, albeit with little or no glacial erosion. Inside the zone of strong valley erosion is a distinct region of scoured terrain that is entirely located on the main plateau surface. This indicates that warm-based ice flowed across the broad low relief granite plateau with plucking and abrasion on rock surfaces resulting in rock basins and intervening rock knobs, roche moutonnée landforms, striated surfaces, and subglacial streamlining resulting in elongated lineations. However, compared to the outlet valleys, less erosion occurred on the plateau surface as indicated by occurrences of preserved saprolites in this landscape. The centrally located zone of preservation is coincident with the area of high topography, the occurrence of a metamorphic sedimentary unit, and minimum erosion

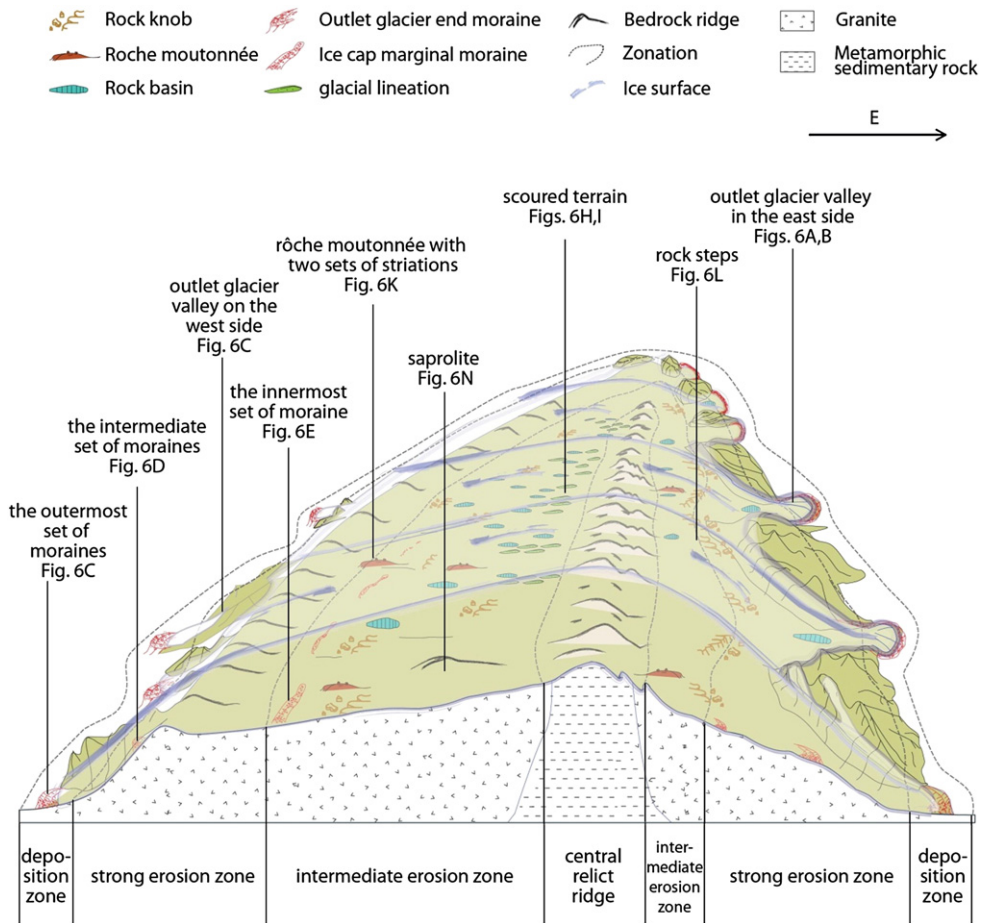


Fig. 7. A model of the asymmetric ice cap in the Haizishan Plateau. Major landscape zones are indicated by the black curved dashed lines. The ice extent is constrained by the outermost distinct set of moraines. The distal border of the deposition zone extends a little farther than the outermost set of moraines, based on observations of dispersed boulders (erratics) beyond the mapped topographic features.

(Fig. 6M), which suggests that it was an area of cold-based ice or otherwise resided underneath the dome or an ice-divide of the ice cap.

The zonal model of landform associations for the Haizishan Plateau is illustrated in Fig. 7, and the asymmetric pattern of the zonation corresponding to the differences between the eastern and western topography of the plateau indicates that the asymmetry may be controlled by topography. The overall zonation is similar to the large-scale patterns of Quaternary ice sheet erosion and deposition in Fennoscandia (Kleman et al., 2008). The presence of saprolite in the ice-scoured landscape indicates a juxtaposition of warm-based and consistently cold-based ice patches, which has also been found in studies of northern hemisphere ice sheets (Sugden and Watts, 1977; Kleman and Stroeven, 1997; Fabel et al., 2002; Harbor et al., 2006). A complex thermal regime is common for continental ice sheets, such as the Fennoscandian Ice Sheet, which covered a large area of over 25° in latitude and 30° in longitude (Kleman et al., 1997). Different climate patterns and diverse underlying topography and geology across such a large area led to the production of varied basal thermal conditions. At the base of the Haizishan Plateau ice cap, cold-based ice across part of the low relief plateau surface, producing limited erosion and deposition, and warm-based ice in the valleys radiating off the plateau margin producing distinctive glacial valleys through large amounts of bedrock erosion. Because the Haizishan ice cap only covered about 4000 km², it is unlikely that distinct climate gradients produced diverse basal thermal patterns, but rather that topographic control was a dominant factor.

The assemblage of glacial landforms and the asymmetric underlying topography provide a somewhat comparable pattern to that found in Fennoscandia, although at a vastly different scale. The Fennoscandian Ice Sheet originated from the central, elongated Scandinavian Mountain range and spread to cover a large area of northern Europe in its southern and eastern sectors. The landscapes it produced include extensive areas of low relief erosional and depositional terrains including many rock basins and lineations. The western margin of the Fennoscandian Ice Sheet posed a contrasting situation, with a shorter distance from the dome of the ice sheet to a marine margin through mountainous terrain, creating deeply carved glacial valleys and troughs with intermediate areas that were either nunataks or covered by nonerosive, cold-based ice (Kleman et al., 2008). At a much smaller scale on the Haizishan

Plateau, but also related to underlying topography, the zonal pattern is asymmetric, reflecting the relatively steep topography to the east of the central high area and a much wider, lower gradient area to the west. Selective linear erosion produced long, deep glacial valleys in the east and short, steep valleys in the west (Figs. 6A, B, C, 7).

In addition to ice maximum conditions, the deposits and landforms also provide insight into the sequence of events that occurred during subsequent glaciations. As the ice retreated to the plateau surface, the ice cap developed into separated smaller icefields controlled by topography. This pattern can be differentiated by patches with distinct landform assemblages related to these ice masses (Fig. 5A), one in the northern part of the plateau, an extensive area associated with scoured terrain and extending farther south, a southwestern region and an eastern region – where sinuous moraines delineate the outline of the separate ice caps or ice fields and valley heads clustering at the ice origins.

7.2. Glacial extent in the Shaluli Shan compared to other regions of the Tibetan Plateau

The minimum extent of maximum glaciation in the Shaluli Shan is about 45,000 km², which represents 43% of the total 104,000 km² area of the Shaluli Shan. Two other areas, centered on the Bayan Har Shan on the northeastern margin of the Tibetan Plateau (Heyman et al., 2008, 2011a; Figs. 10, 11) and the Tanggula Shan on the central Tibetan Plateau (Morén et al., 2011; Figs. 10, 11), have been mapped using a similar consistent methodology and the same data sources. In comparison to the Shaluli Shan area, both the other areas have, on average, higher topography and less relief including more extensive intact low relief plateau surfaces. Abundant glacial depositional and erosional landforms occur within and surrounding the mountain ranges in these two areas, but they lack evidence for more extensive ice cap glaciation across the extensive low relief plateau surfaces. As Fig. 8 shows, the hypsometry of the formerly glaciated landscape of the Shaluli Shan extends to lower elevations than in the Bayan Har Shan and the Tanggula Shan areas. Moreover, the hypsometric curve exhibits a more even distribution in the Shaluli Shan than in the other areas.

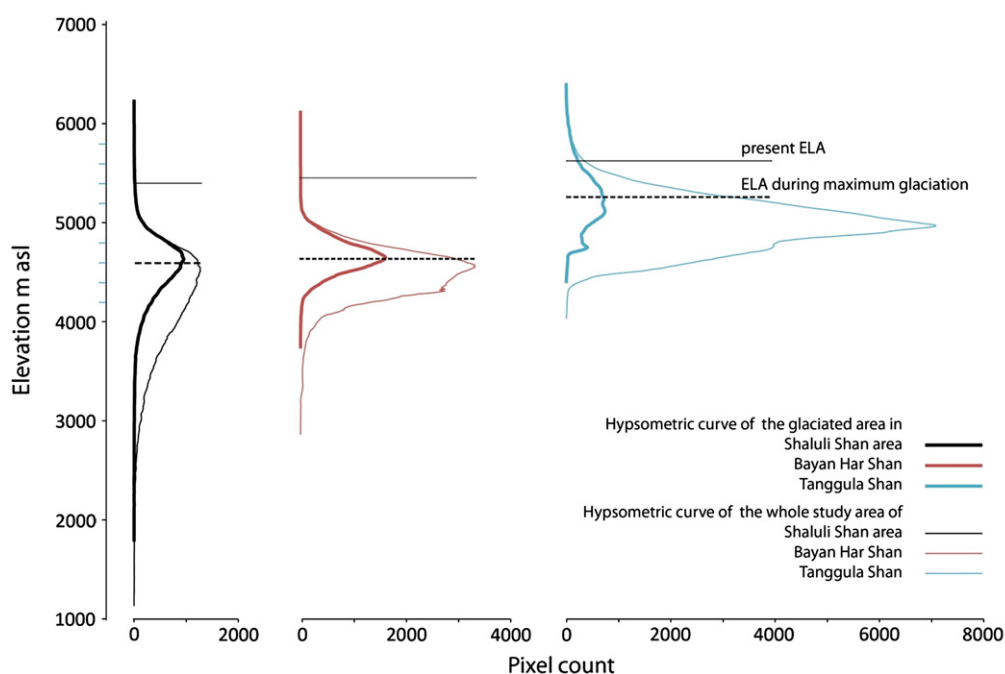


Fig. 8. Hypsometric curves for the formerly glaciated landscape portions and for the whole study area of the three regions with detailed glacial landform mapping. The horizontal black lines and dashed black lines indicate the equilibrium line altitude (ELA) of present and maximum glaciation, respectively, based on estimations published in Shi et al. (2000).

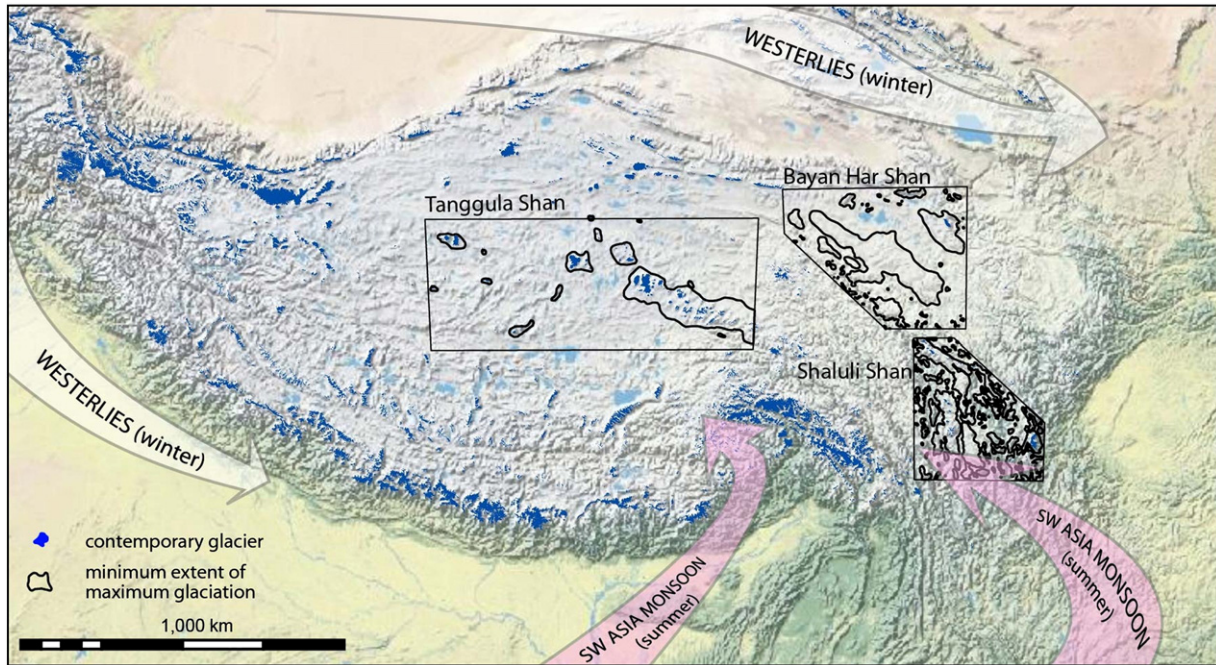


Fig. 9. Minimum extent of maximum glaciation on the eastern and central Tibetan Plateau was reconstructed from detailed geomorphological mapping of glacial landforms: (Tanggula Shan from Morén et al. (2011); Bayan Har Shan from Heyman et al. (2009); Shaluli Shan from Fu et al. (2012). The arrows denote modern dominant pathways for winter precipitation (westerlies) and summer precipitation (SW Asia monsoon) (adapted from Benn and Owen, 1998).

The differences in patterns of Quaternary glaciation among the three regions may be explained by the climatology and topography (Fig. 9). The majority of the annual precipitation in the Shaluli Shan is provided by the summer monsoon, while winter westerlies provide

relatively little precipitation (Shi et al., 2006). The moist summer monsoon precipitation-bearing winds must cross high relief areas, including the Hengduan Mountain Range (including the Shaluli Shan), before they can penetrate farther north and west to the Bayan Har

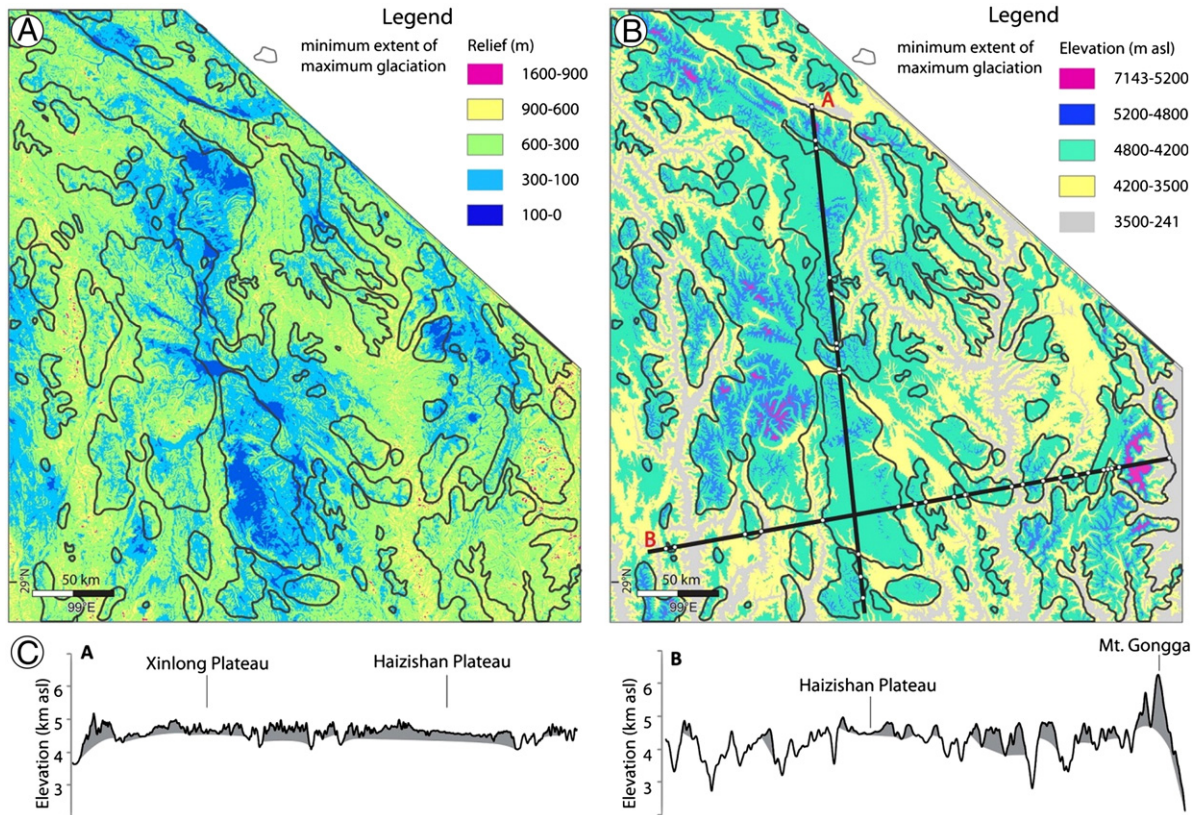


Fig. 10. Reconstructed minimum extent of maximum glaciation projected on top of (A) relief map (derived from ~90-m DEM calculated over a circular domain with radius of 500 m) and (B) DEM of the Shaluli Shan area. (C) Topographic profiles of transects A and B, where the shaded gray is glaciated area (see panel B for the locations of the transects).

Shan and Tanggula Shan, respectively (Fig. 9). During periods of maximum glaciation, the ELA depression was more pronounced in the Shaluli Shan and the Bayan Har Shan than in the Tanggula Shan area. The resultant, larger proportion of topography above the ELA allowed for a higher proportion of the glaciated area relative to the total area. The Haizishan and Xinlong Plateaus, with significant low relief plateau surfaces above the ELA, tended to host extensive ice caps. Such conditions with ice caps on low relief plateau surfaces did not occur in the other study areas.

7.3. Topographic controls on the Haizishan Ice Cap

In addition to precipitation, discussed above, topography is another important controlling factor for ice cap growth on the Haizishan Plateau. Both areas are characterized by extensive surfaces of low relief, <300 m, and high elevation, >4200 m asl (Fig. 10). Clark et al. (2006) interpreted low relief areas of the Tibetan Plateau, including both plateaus in the Shaluli region, as paleo landscapes that were formed at low elevations and then uplifted by tectonic forces with only minor surface disruption by fluvial incision. The low relief plateaus in the Shaluli Shan area with glacial imprints of ice caps are located above 4200 m asl (Fig. 10), and the majority of the surface area is between 4400 and 4800 m asl. An ELA drop to 4600 m asl during maximum glaciation (Shi et al., 2000; Fig. 10) allowed for rapid buildup of ice across a broad area of the Haizishan and Xinlong Plateaus (Instantaneous glacierization; Ives, 1957); and growth of ice caps, while areas with peaks above 4600 m asl but lacking plateau surfaces at or above the threshold of 4600 m asl only developed valley glaciers.

At a larger scale, the reconstructed glaciated areas tend to connect longitudinally, forming large blocks, but are fragmented latitudinally (Fig. 10). This pattern is considered to reflect the topography, which is more uniform longitudinally but dissected latitudinally, because of lateral expansion of the Tibetan Plateau (Clark et al., 2005). Furthermore, the longitude profile A in Fig. 10 exhibits little variation of the low limits of the reconstructed glaciated area, while the latitude profile B presents a trend of east-westerly elevated low limits of the glaciated area. This is probably caused by more rapid weakening of the Southwest Asian monsoon because of blocking by high mountains while longitudinally extending river gorges enable the Southwest Asian monsoon to penetrate this region more effectively. In addition, in profile B (Fig. 10), the glaciated area reach is lower on the east slope than on the west slope, implying higher accumulation of snow on the east slope.

8. Conclusions

Detailed glacial geomorphological mapping and field investigations of the Shaluli Shan on the southeastern Tibetan Plateau indicate:

Multiple episodes of glaciation occurred in the Shaluli Shan. The minimum extent of maximum Quaternary glaciation covers 43% of the mapped area of 104,000 km².

The glacial landforms of the Haizishan and Xinlong Plateaus were formed by ice caps with outlet glaciers; glaciation elsewhere in the study area was alpine in style.

A zonal distribution of landforms associated with the Haizishan ice cap similar to that created by mid-latitude northern hemisphere ice sheets.

The zonation of glacial landforms suggests that the Haizishan ice cap had a complex basal thermal regime.

Topography played a major role in the asymmetric pattern of glacial landform development in the Haizishan Plateau.

The glaciations of the Shaluli Shan area reached lower altitudes than other areas of the Tibetan Plateau that have been mapped in similar detail and with similar methodology. This is likely a result of both precipitation patterns and topographic factors.

Acknowledgments

We thank Emma Johansson, Jun Feng, Barbara Heyman, and Björn Morén for the field assistance. Funding for fieldwork and group workshops was provided by the Swedish Research Council/Swedish International Development Cooperation Agency (VR/SIDA) through their Swedish Research Links programme to Stroeven (No. 348-2007-6924) and by Purdue University.

Appendix A. Supplementary data

Supplementary data associated with this article can be found in the online version, at <http://dx.doi.org/10.1016/j.geomorph.2012.10.030>. These data include Google maps of the most important areas described in this article.

References

- Benn, D.I., Evans, D.J.A., 2010. Glaciers and Glaciation, 2nd edition. Elsevier, London, pp. 473–527.
- Benn, D.I., Owen, L.A., 1998. The role of the Indian summer monsoon and the mid-latitude westerlies in Himalayan glaciation: review and speculative discussion. *Journal of the Geological Society* 155 (2), 353–363.
- Boulton, G.S., Clark, C.D., 1990. A highly mobile Laurentide ice sheet revealed by satellite images of glacial lineations. *Nature* 346 (6287), 813–817.
- Brantley, S.L., White, A.F., 2009. Approaches to modeling weathered regolith. *Reviews in Mineralogy and Geochemistry* 70 (1), 435–484.
- Butt, C.R.M., Lintern, M.J., Anand, R.R., 1997. Evolution of regoliths and landscapes in deeply weathered terrain – implications for geochemical exploration. *Ore Geology Reviews* 16, 167–183.
- Clark, M.K., House, M.A., Royden, L.H., Whipple, K.X., Burchfiel, B.C., Zhang, X., Tang, W., 2005. Late Cenozoic uplift of southeastern Tibet. *Geology* 33 (6), 525–528.
- Clark, M.K., Royden, L.H., Whipple, K.X., Burchfiel, B.C., Zhang, X., Tang, W., 2006. Use of a regional, relict landscape to measure vertical deformation of the eastern Tibetan Plateau. *Journal of Geophysical Research* 111 (F3), F03002.
- Cui, Z.J., 1964. On the problem of Pleistocene icecover patterns in west China. *Acta Geologica Sinica* 44, 2–6 (in Chinese, English abstract).
- Cui, Z.J., 1979. Classification of the Glaciations in the western China and its basis. *Acta Geologica Sinica* 1 (2), 13–21 (in Chinese, English abstract).
- Cui, Z.J., 1981a. Glacial erosion landforms and development of trough at the head of Urumqi River, Tian Shan. *Journal of Glaciology and Geocryology* 3, 1–15 (in Chinese, English abstract).
- Cui, Z.J., 1981b. Cirques at the head of Urumqi River, Tian Shan. *Journal of Glaciology and Geocryology* 3, 24–25 (in Chinese, English abstract).
- Derbyshire, E., Shi, Y., Li, J., Zheng, B., Li, S., Wang, J., 1991. Quaternary glaciation of Tibet: the geological evidence. *Quaternary Science Reviews* 10 (6), 485–510.
- Fabel, D., Stroeve, A.P., Harbor, J., Kleman, J., Elmore, D., Fink, D., 2002. Landscape preservation under Fennoscandian ice sheets determined from in situ produced ¹⁰Be and ²⁶Al. *Earth and Planetary Science Letters* 201 (2), 397–406.
- Fu, P., Heyman, J., Hätteström, C., Stroeve, A.P., Harbor, J., 2012. Glacial geomorphology of the Shaluli Shan, southeastern Tibetan Plateau. *Journal of Maps* 8 (1), 48–55.
- GLCF, 2011. Global Land Cover Facility. Retrieved in May 2010, from <http://www.landcover.org>.
- Graf, A.A., Strasky, S., Zhao, Z.Z., Akçar, N., Ivy-Ochs, S., Kubik, P.W., Christl, M., Kasper, H.U., Wielert, R., Schlüchter, C., 2008. Glacier extension on the eastern Tibetan Plateau in response to MIS 2 cooling, with a contribution to ¹⁰Be and ²¹Ne methodology. In: Strasky, S. (Ed.), *Glacial response to global climate changes: cosmogenic nuclide chronologies from high and low latitudes*. PhD Thesis, ETH Zürich. University of Bern, Bern, pp. 77–110.
- Harbor, J., Stroeve, A.P., Fabel, D., Clarhäll, A., Kleman, J., Li, Y., Elmore, D., Fink, D., 2006. Cosmogenic nuclide evidence for minimal erosion across two subglacial sliding boundaries of the late glacial Fennoscandian ice sheet. *Geomorphology* 75 (1–2), 90–99.
- Harrison, T.M., Copeland, P., Kidd, W.S.F., Yin, A., 1992. Raising Tibet. *Science in China Series B-Chemistry* 255 (5052), 1663–1670.
- Hedin, S., 1909. *Trans-Himalaya*. Macmillan, New York. (1–427 pp.).
- Hedin, S., 1922. *Southern Tibet*. Lithographic Institute of the General Staff of the Swedish Army, Stockholm, pp. 3–421.
- Heyman, J., Hätteström, C., Stroeve, A.P., 2008. Glacial Geomorphology of the Bayan Har sector of the NE Tibetan plateau. *Journal of Maps* 2008, 42–62.
- Heyman, J., Stroeve, A.P., Alexanderson, H., Hätteström, C., Harbor, J., Li, Y.K., Caffee, M.W., Zhou, L.P., Veres, D., Liu, F., Machiedo, M., 2009. Paleoglacieration of Bayan Har Shan, northeastern Tibetan Plateau: glacial geology indicates maximum extents limited to ice cap and ice field scales. *Journal of Quaternary Science* 24 (7), 710–727.
- Heyman, J., Stroeve, A.P., Harbor, J.M., Caffee, M.W., 2011a. Too young or too old: evaluating cosmogenic exposure dating based on an analysis of compiled boulder exposure ages. *Earth and Planetary Science Letters* 302 (1–2), 71–80.
- Heyman, J., Stroeve, A.P., Caffee, M.W., Hätteström, C., Harbor, J., Li, Y.K., Alexanderson, H., Zhou, L.P., Hubbard, A., 2011b. Palaeoglaciology of Bayan Har Shan, NE Tibetan

- Plateau: exposure ages reveal a missing LGM expansion. *Quaternary Science Reviews* 30 (15–16), 1988–2001.
- Huntington, E., 1906. Pangong: a glacial lake in the Tibetan Plateau. *Journal of Geology* 14, 599–617.
- Ives, J.D., 1957. Glaciation of the Torngat Mountains, northern Labrador. *Arctic* 10 (2), 67–86.
- Jarvis, A., Reuter, H.I., Nelson, A., Guevara, E., 2008. Hole-filled Seamless SRTM Data V4. International Centre for Tropical Agriculture. Retrieved in August 2009, from <http://srtm.csi.cgiar.org>.
- Kleman, J., Stroeven, A.P., 1997. Preglacial surface remnants and Quaternary glacial regimes in northwestern Sweden. *Geomorphology* 19 (1–2), 35–54.
- Kleman, J., Hätestrand, C., Borgström, I., Stroeven, A.P., 1997. Fennoscandian paleoglaciology reconstructed using a glacial geological inversion model. *Journal of Glaciology* 43, 283–299.
- Kleman, J., Stroeven, A.P., Lundqvist, J., 2008. Patterns of Quaternary ice sheet erosion and deposition in Fennoscandia and a theoretical framework for explanation. *Geomorphology* 97 (1–2), 73–90.
- Klinge, M., Lehmkühl, F., 2004. Pleistocene glaciations in southern and eastern Tibet. In: Ehlers, J., Gibbard, P.L. (Eds.), *Quaternary Glaciations – Extent and Chronology, Part III: South America, Asia, Africa, Australasia, Antarctica*. Elsevier, Amsterdam, pp. 361–369.
- Kuhle, M., 1986. The upper limit of glaciation in the Himalayas. *GeoJournal* 13, 331–346.
- Kuhle, M., 1987. The Problem of a Pleistocene inland glaciation of the Northeastern Qinghai-Xizang Plateau. In: Hövermann, J., Wang, W. (Eds.), *Reports of the Qinghai-Xizang (Tibet) Plateau*, Beijing, pp. 250–315 (in Chinese).
- Kuhle, M., 1988. Geomorphological findings on the built-up of Pleistocene glaciation in Southern Tibet and on the problem of inland ice. *GeoJournal* 17, 457–512.
- Kuhle, M., 1990. Ice marginal ramps and alluvial fans in semiarid mountains: convergence and difference. In: Rachočí, A.H., Church, M. (Eds.), *Alluvial Fans: A Field Approach*. Wiley, Chichester, pp. 55–68.
- Kuhle, M., 1991. Observations supporting the Pleistocene inland glaciations of High Asia. *GeoJournal* 25, 131–231.
- Kuhle, M., 1995. Glacial isostatic uplift of Tibet as a consequence of a former ice sheet. *GeoJournal* 37, 431–449.
- Lehmkuhl, F., Liu, S., 1994. An outline of physical geography including Pleistocene glacial landforms of Eastern Tibet (provinces Sichuan and Qinghai). *GeoJournal* 34 (1), 7–30.
- Lehmkuhl, F., Owen, L.A., 2005. Late Quaternary glaciation of Tibet and the bordering mountains: a review. *Boreas* 34 (2), 87–100.
- Lehmkuhl, F., Owen, L.A., Derbyshire, E., 1998. Late Quaternary glacial history of northeast Tibet. *Quaternary Proceedings* 6, 121–142.
- Li, J.J., 1975. Recent study on glaciers in southeast Xizang. *Journal of Lanzhou University* 2, 53–57 (in Chinese).
- Li, J.J., Xu, S., 1983. Morphology development and Quaternary Glaciations in north Pakistan. *Acta Geographica Sinica* 38 (1), 11–24 (in Chinese, English abstract).
- Li, B.Y., Wang, F.B., Zhang, Q.S., Yang, Y.T., Yin, Z., Jil, K., 1983. *Quaternary Geology of Xizang*. Science Press, Beijing, pp. 1–192 (in Chinese).
- Li, B.Y., Li, J.J., Cui, Z.J., Zheng, B.X., Zhang, Q.S., Wang, F.B., Zhou, S.Z., Shi, Z.H., Jiao, K.Q., KANG, J.C., 1991. Quaternary glacial distribution map of Qinghai-Xizang (Tibet) plateau. Science Press, Beijing, Mapscale 1:3,000,000 (in Chinese).
- Li, J.J., Feng, Z., Zhou, S.Z., 1996. The Quaternary glacial remnants in Hengduan Mountain. In: Li, J.J., Su, Z. (Eds.), *Glaciers in Hengduan Mountains*. Science Press, Beijing, pp. 157–212 (in Chinese).
- Lidmar-Bergström, K., 1995. Relief and saprolites through time on the Baltic Shield. *Geomorphology* 12 (1), 45–61.
- Luo, L., Yang, Y., 1963. An approach of geomorphological formation in the region of West Sichuan and North Yunnan. *Geographical Bulletin* 5, 34–46 (in Chinese).
- Morén, B., Heyman, J., Stroeven, A.P., 2011. Glacial geomorphology of the central Tibetan Plateau. *Journal of Maps* 2011, 115–125.
- Ouimet, W., Whipple, K., Royden, L., Reiners, P., Hodges, K., Pringle, M., 2010. Regional incision of the eastern margin of the Tibetan Plateau. *Lithosphere* 2 (1), 50–63.
- Owen, L.A., Finkel, R.C., Caffee, M.W., Gualtieri, L., 2002. Timing of multiple late Quaternary glaciations in the Hunza Valley, Karakoram Mountains, northern Pakistan: defined by cosmogenic radionuclide dating of moraines. *Geological Society of America Bulletin* 114 (5), 593–604.
- Owen, L.A., Finkel, R.C., Haizhou, M., Spencer, J.Q., Derbyshire, E., Barnard, P.L., Caffee, M.W., 2003. Timing and style of Late Quaternary glaciation in northeastern Tibet. *Geological Society of America Bulletin* 115 (11), 1356–1364.
- Owen, L.A., Finkel, R.C., Barnard, P.L., Ma, H.Z., Asahi, K., Caffee, M.W., Derbyshire, E., 2005. Climatic and topographic controls on the style and timing of Late Quaternary glaciation throughout Tibet and the Himalaya defined by ^{10}Be cosmogenic radionuclide surface exposure dating. *Quaternary Science Reviews* 24 (12–13), 1391–1411.
- Owen, L.A., Caffee, M.W., Finkel, R.C., Seong, Y.B., 2008. Quaternary glaciation of the Himalayan–Tibetan orogen. *Journal of Quaternary Science* 23 (6–7), 513–531.
- Rutter, N., 1995. Problematic ice sheets. *Quaternary International* 28, 19–37.
- Schäfer, J.M., Tschudi, S., Zhao, Z., Wu, X., Ivy-Ochs, S., Wieler, R., Baur, H., Kubik, P.W., Schlüchter, C., 2002. The limited influence of glaciations in Tibet on global climate over the past 170 000 yr. *Earth and Planetary Science Letters* 194 (3–4), 287–297.
- Shi, Y.F., 1992. Glaciers and glacial geomorphology in China. *Zeitschrift für Geomorphologie* 86, 19–35.
- Shi, Y.F., Liu, T., 1964. Preliminary report on the Mt. Xixabangma Scientific Expedition. *Scientia Sinica* 10, 928–938 (in Chinese).
- Shi, Y.F., Cui, Z.J., Zheng, B., 1982. Inquiry on ice ages in Mount Xixabangma Region. In: Shi, Y.F., Liu, D.S. (Eds.), *Reports of Scientific Expedition in Mount Xixabangma Region*. Science Press, Beijing, pp. 155–176 (in Chinese).
- Shi, Y.F., Ren, B., Wang, J., Derbyshire, E., 1986. Quaternary glaciation in China. *Quaternary Science Reviews* 5, 503–507.
- Shi, Y.F., Zheng, B.X., Li, S.J., 1992. Last glaciation and maximum glaciation in the Qinghai-Xizang (Tibet) Plateau: a controversy to M. Kuhle's ice sheet hypothesis. *Zeitschrift für Geomorphologie* 84, 19–35.
- Shi, Y.F., Zheng, B.X., Su, Z., 2000. The glacial and interglacial cycles and environment changes during Quaternary. In: Shi, Y.F. (Ed.), *Glaciers and their environments in China—the present, past and future*. Hebei Science and Technology Publishing House, Hebei, pp. 323–341 (in Chinese).
- Shi, Y.F., Cui, Z.J., Su, Z., 2005. *The Quaternary Glaciations and Environmental Variations in China*. Hebei Science and Technology Publishing House, Hebei, pp. 320–352 (in Chinese, English abstract).
- Shi, Y.F., Zheng, B.X., Su, X., 2006. Quaternary glacier, glaciations and interglacial oscillations and environmental change. In: Shi, Y.F., Cui, Z.J., Su, Z. (Eds.), *The Quaternary Glaciations and Environmental Variations in China*. Hebei Science and Technology Publishing House, Hebei, pp. 65–103 (in Chinese).
- Shi, Y.F., Zhao, J.D., Wang, J., 2011. New understanding of Quaternary Glaciations in China. Shanghai Popular Science Press, Shanghai, pp. 84–89 (in Chinese).
- Sinitius, V.M., 1958. On the problem of Quaternary Glaciation of High Asia Plateau. *Geographical Translations*. Science Press, Beijing, pp. 22–27.
- Strasky, S., Graf, A.A., Zhao, Z., Kubik, P.W., Baur, H., Schlüchter, C., Wieler, R., 2009. Late Glacial ice advances in southeast Tibet. *Journal of Asian Earth Sciences* 34 (3), 458–465.
- Stroeven, A.P., Hätestrand, C., Heyman, J., Harbor, J., Li, Y.K., Zhou, L.P., Caffee, M.W., Dong, J.Y., Alexanderson, H., Kleman, J., Ma, H.Z., Liu, G.N., 2009. Landscape analysis of the Huang He headwaters, NE Tibetan Plateau – glacial and fluvial erosion patterns. *Geomorphology* 103 (2), 212–226.
- Stroeven, A.P., Harbor, J., Heyman, J., Liu, G.N., 2011. Glacial Erosion Landscapes. In: Schroder, J., Giardino, R., Harbor, J. (Eds.), *Treatise on Geomorphology*, pp. 212–226.
- Sugden, D.E., John, B.S., 1976. *Glaciers and Landscape*. Edward Arnold, London, pp. 151–191.
- Sugden, D.E., Watts, S.H., 1977. Tors, felsenmeere and glaciation in the northern Cumberland Peninsula. Baffin Island. *Canadian Journal of Earth Sciences* 14, 2817–2823.
- Trinkler, E., 1930. The ice age on the Tibetan Plateau and in the adjacent regions. *The Geographical Journal* 75, 225–232.
- Wang, J., Raisbeck, G., Xu, X., You, F., Bai, S., 2006. In situ cosmogenic ^{10}Be dating of the Quaternary glaciations in the southern Shaluli Mountain on the Southeastern Tibetan Plateau. *Science in China Series D: Earth Sciences* 49 (12), 1291–1298.
- Wang, J., Zhou, S., Zhao, J., Zheng, J., Guo, X., 2011. Quaternary glacial geomorphology and glaciations of Kongur Mountain, eastern Pamir, China. *Science China Earth Sciences* 54 (4), 591–602.
- Ward, F.K., 1922. The glaciation of Chinese Tibet. *The Geographical Journal* 59, 363–369.
- Ward, F.K., 1934. The Himalaya east of the Tsangpo. *The Geographical Journal* 84, 363–397.
- Xu, L.B., Zhou, S.Z., 2009. Quaternary glaciations recorded by glacial and fluvial landforms in the Shaluli Mountains, Southeastern Tibetan Plateau. *Geomorphology* 103 (2), 268–275.
- Xu, L.B., Ou, X.J., Lai, Z.P., Zhou, S.Z., Wang, J., Fu, Y.C., 2010. Timing and style of Late Pleistocene glaciation in the Queer Shan, northern Hengduan Mountains in the eastern Tibetan Plateau. *Journal of Quaternary Science* 25 (6), 957–966.
- Zheng, B.X., 1989. Controversy regarding the existence of a large ice sheet on the Qinghai-Xizang (Tibetan) Plateau during the Quaternary Period. *Quaternary Research* 32, 121–123.
- Zheng, B.X., 2000. Quaternary glaciation and glacier evolution in the Yulong Mount, Yunan. *Journal of Glaciology and Geocryology* 22 (1), 54–61 (in Chinese, English abstract).
- Zheng, B.X., 2001. Study on the quaternary glaciation and the formation of the Moxi platform in the east slopes of the Mount Gongga. *Journal of Glaciology and Geocryology* 23 (3), 283–291 (in Chinese, English abstract).
- Zheng, B.X., 2002. Quaternary Glaciation and Glacier Evolution in the Yulong Mount, Yunan. *Journal of Glaciology and Geocryology* 22 (1), 54–61.
- Zheng, B.X., 2006. Quaternary glaciations in the Hengduan Mountains. In: Shi, Y.F., Cui, Z.J., Su, Z. (Eds.), *The Quaternary Glaciations and Environmental Variations in China*. Hebei Science and Technology Publishing House, pp. 407–441 (in Chinese, English abstract).
- Zheng, B.X., Ma, Q.H., 1994. The development of glacier fluctuations, climate changes and fluvial valley in Gongga Shan in the Holocene. *Acta Geographica Sinica* 49 (6), 400–508 (in Chinese).
- Zheng, B.X., Ma, Q.H., 1995. A study on the geomorphological characteristics and glaciations in Paleo-Daocheng Ice Cap, western Sichuan. *Journal of Glaciology and Geocryology* 17, 23–32 (in Chinese).
- Zheng, B.X., Rutter, N., 1998. On the problem of Quaternary glaciations, and the extent and patterns of Pleistocene ice cover in the Qinghai-Xizang (Tibet) Plateau. *Quaternary International* 45–46, 109–122.
- Zheng, B.X., Shi, Y.F., 1976. On Quaternary Glaciation of Mount Qomolangma Area. In: C.A.O.S. (Ed.), *Comprehensive Scientific Expedition to the Qinghai-Xizang Plateau. Reports of Qomolangma Area Scientific Expedition (1966–1968)*. Science Press, Beijing, pp. 29–62 (in Chinese).
- Zheng, B.X., Li, J.J., 1981. Quaternary glaciations on the Qinghai-Xizang Plateau. *Proceedings of International Symposium on the Qinghai-Xizang (Tibetan Plateau) Geological and Ecological Research* 1, pp. 1631–1640 (in Chinese).
- Zheng, B.X., Xu, Q., Shen, Y.P., 2002. The relationship between climate change and Quaternary glacial cycles on the Qinghai-Tibetan Plateau: review and speculation. *Quaternary International* 97–98, 93–101.
- Zhou, S.Z., Li, J.J., 1998. The sequence of Quaternary glaciation in the Bayan Har Mountains. *Quaternary International* 45–46, 135–142.
- Zhou, S.Z., Xu, L.B., Colgan, P.M., Mickelson, D.M., Wang, X.L., Wang, J., Zhong, W., 2007. Cosmogenic ^{10}Be dating of Guxiang and Baiyu glaciations. *Chinese Science Bulletin* 52, 1387–1393.